

Matrix Isolation of H Atoms at Low Temperatures

V.V. Khmelenko · D.M. Lee · S. Vasiliev

Received: 11 June 2010 / Accepted: 15 November 2010 / Published online: 3 December 2010
© Springer Science+Business Media, LLC 2010

Abstract The recent history of the matrix isolation of atomic free radicals at low temperatures started with a research program at the US National Bureau of Standards and continued with the important breakthrough at Chernogolovka in Russia where a jet containing atomic free radicals was directed onto the surface of superfluid ^4He . The samples collected consisted of gel-like substances made up of molecular nanoclusters, allowing the atomic free radicals to be isolated from one another and studied at 1.3 K. More recently, techniques were developed at Turku University which have been made the region $T < 1$ K accessible for studies of H atoms entrapped in H_2 films. Very high concentrations of H atomic free radicals ($\sim 10^{18}$ – 10^{19} cm^{-3}) have been attained using both the Turku and Chernogolovka methods. A discussion of the most recent experiments at Cornell and Turku will be given. Microwave and mm wave electron paramagnetic resonance techniques have been employed in these experiments. These techniques permitted studies of the exchange tunneling chemical reaction $\text{D} + \text{HD} \rightarrow \text{H} + \text{D}_2$. Diffusion of H atoms through solid H_2 proceeds via the reaction $\text{H} + \text{H}_2 \rightarrow \text{H}_2 + \text{H}$, leading to recombination ($\text{H} + \text{H} \rightarrow \text{H}_2$). Quantum overlap of H atoms is thought to be responsible for exotic behavior of H atoms in solid H_2 films below 1 K, including a significant departure from the Boltzmann distribution of the relative populations of the two lowest hyperfine levels of atomic H.

V.V. Khmelenko (✉) · D.M. Lee
Department of Physics and Astronomy, Texas A&M University, College Station, TX, 77843, USA
e-mail: khmel@physics.tamu.edu

D.M. Lee
Department of Physics, Cornell University, Ithaca, NY, 14853, USA

S. Vasiliev
Wihuri Physical Laboratory, Department of Physics and Astronomy, University of Turku,
20014 Turku, Finland

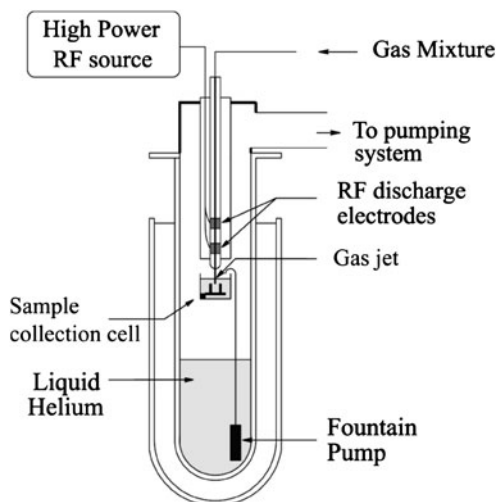
Keywords Atomic and molecular hydrogen · Matrix isolation · Free radicals · Electron spin resonance

1 Introduction and Background

The story begins in the late 1950s when a research program was initiated at the US National Bureau of Standards (now the National Institute of Standards and Technology) to investigate matrix isolated free radicals at low temperatures. The motivation for these investigations was to develop a powerful chemical rocket fuel. A wide range of techniques was applied in these studies, including optical spectroscopy, electron spin resonance (ESR), A.C. susceptibility, and thermodynamic measurements. The main method of sample preparation was to condense the products of a radio-frequency discharge containing the species to be studied onto a cold surface. For example, gaseous molecular nitrogen was passed through the discharge, which dissociated a large fraction of the molecules into atomic nitrogen, which was then cryopumped onto the liquid helium cooled surface. The result was a sample of solid molecular nitrogen with embedded N atoms. Alas, the concentrations of the N atom free radicals obtained were far too small to provide the required energy storage. The loss of N atoms was attributed to rapid recombination during the deposition process. Similar experiments were also performed on hydrogen. Although the research program did not achieve its stated goals, a great deal of knowledge was obtained during the course of the investigations, as provided in a comprehensive volume edited by Bass and Broida [1].

Following these studies, relatively little attention was devoted to further investigations of matrix isolated free radicals until a revolutionary development took place in Chernogolovka, Russia by Gordon, Mezhov-Deglin and Pugachev [2]. Instead of condensing the discharge products onto a helium cooled surface, they condensed the sample directly into a beaker of liquid helium maintained at a temperature well below the lambda point (see Fig. 1). The superfluid level in the beaker was maintained by a fountain pump, which was connected to the main liquid helium bath situated below the beaker. As the gas left the discharge region, it passed through a small orifice, causing a jet to be formed. A crater or depression could be observed where the jet impacted the superfluid helium surface. For the case of the nitrogen samples, a green glow was seen to emanate from the sample, which appeared as a translucent gel-like substance. Spectroscopic studies performed on these samples indicated a strong signal from the $^2D-^4S$ forbidden line of atomic nitrogen as manifested by the green glow, which persisted for several minutes [3]. This observation indicated the presence of a large concentration of N atoms. This conclusion was soon reinforced by ESR studies of the samples by Gordon et al. [4]. Quantitative ESR studies showed that 10^{20} N atoms per cm^3 could be produced in the samples, a spectacular improvement from earlier studies. The dipolar broadened ESR line widths observed in these experiments not only enabled the N atom concentrations to be determined, but also gave a powerful indication that interactions between the atomic free radicals could be studied and might reveal new and interesting phenomena. The structure of these samples was determined from x-ray diffraction experiments by Kiryukhin et al. [5],

Fig. 1 Experimental setup for preparation of impurity-helium condensates



and showed conclusively that they were gels composed of many small nanoclusters. These gels were given the names, “Impurity Helium Condensates,” or “Impurity Helium Solids.”

Later work was carried out at Cornell University. Further structural studies using ultrasound techniques showed that the interstices or channels in the porous structures were occupied by superfluid helium and ranged in size from 8 to 860 nm [6]. Further ESR experiments at Cornell were devoted to studies of exchange tunneling chemical reactions in hydrogen-deuterium mixtures, which had first been revealed in experiments at Chernogolovka [7] and later at the Kurchatov Institute by Lukashevich’s group [8]. Two reactions were involved. A fast initial reaction corresponded to a D atom interacting with an H₂ molecule to form a hydrogen atom and an HD molecule [9]. A second, slower reaction involved a D atom interacting with an HD molecule to form a hydrogen atom and a deuterium molecule. Such interactions led to rather large H atom concentrations ($\sim 10^{18}$ H atoms per cm³) [10]. Miyazaki and his group [11] also studied these reactions in large crystals rather than nanoclusters. The H₂ and D₂ molecules in their samples were dissociated in situ via gamma ray bombardment. The rate constants determined by Miyazaki’s group were in qualitative and, at times, fairly good quantitative agreement with those found in the Cornell experiments. The tunneling mechanism is also thought to be responsible for the recombination reaction $H + H \rightarrow H_2 + 4.8 \text{ eV}$.

Two classes of quantum diffusion were considered in trying to explain the above-mentioned reactions. The first of these involved atoms finding the minimum potential barrier height in the molecular lattice to be overcome by changing positions [12]. For an atomic free radical, this was thought to be ~ 100 K. The potential barrier for the exchange tunneling chemical reaction is significantly larger (~ 5000 K), but the barrier was thought to be narrower for this latter case. The controversy was resolved by experiments performed by Kumada [13], who measured the pressure dependence of the reaction rates. The result agreed well with the exchange tunneling reaction hypothesis, which predicted a minimal pressure dependence of the reaction rate.

Pulsed ESR experiments by Bernard et al. [14] on D atoms embedded in solid D₂ clusters showed that a large fraction of the atomic free radicals were situated on the surfaces of the clusters (diameters ~ 10 nm). The pulse technique employed in this work was “Electron Spin Echo Envelope Modulation,” or ESEEM. The echo amplitude associated with a typical $\pi/2 - \tau - \pi$ -echo pulse sequence was monitored as a function of τ . The decay pattern exhibited by the envelope of successive echo amplitudes as τ increased provided information on the average environment in which D atoms were located. It was thus possible to distinguish between surface populations and populations of atoms deep inside the clusters by this technique. (More neighbors lead to larger envelope modulation.)

Another extremely important technique developed over a period of time at the Kurchatov Institute [8] and later at Turku University in Finland [15] has been the application of millimeter wave spectroscopy. A rather sophisticated 2 mm wave (~ 130 GHz) spectrometer was developed at Turku. Most of the components, including mixers and IF (intermediate frequency) amplifiers, were in the cryogenic region, which improved the signal to noise (S/N) ratio. Shorter low level signal paths also were quite helpful in this regard. The applied magnetic field for H atomic free radicals at this frequency is approximately 4.6 Tesla. It was therefore quite suitable for studying spin polarized hydrogen gas, as well as atomic hydrogen free radicals embedded in solid hydrogen films. Experiments could be carried out to temperatures below 100 mK with the aid of ³He–⁴He dilution refrigerators. The hydrogen molecules were cryopumped into the low temperature regime ($\lesssim 0.5$ K), where they were dissociated and then transported into the sample cell, which contained a Fabry-Perot resonator consisting of a flat mirror and a spherical mirror or two spherical mirrors. An auxiliary helical resonator was placed in the cell for the purpose of observing the ~ 900 MHz transition between the two lowest hyperfine levels. In later experiments this auxiliary helical resonator was also used to dissociate hydrogen atoms directly in the sample cell.

In the following section, recent work at Cornell and Turku on H atoms embedded in H-Kr nanoclusters and in H₂ films will be discussed.

2 Recent Developments

During the past few years, progress has been made on studies of hydrogen atoms embedded in impurity helium condensates consisting of krypton nanoclusters surrounded by layers of solid molecular hydrogen. Although very large signals from H atoms in these samples were first noted in pulsed ESR studies [14] and SQUID susceptibility measurements [16] at Cornell, it turned out that CW ESR provided much more detailed information on this system [17]. The investigations were performed with a 9 GHz (X band) CW spectrometer. The resonant cylindrical cavity operated in the TE₀₁₁ mode, thereby providing access for the sample tube, which was inserted from above as shown in Fig. 2. The cylindrical walls of the cavity were composed of conducting rings electrically insulated from one another to allow passage of a 100 kHz field modulation supplied by auxiliary coils external to the cavity. This allowed lock-in detection of the microwave absorption signal while the main applied field (~ 0.3 Tesla) was swept slowly through a resonance line of the sample. This led

Fig. 2 Low temperature insert used in the ESR investigation of impurity-helium condensates. The quartz beaker is lowered into ESR resonant cavity for measurements after sample preparation

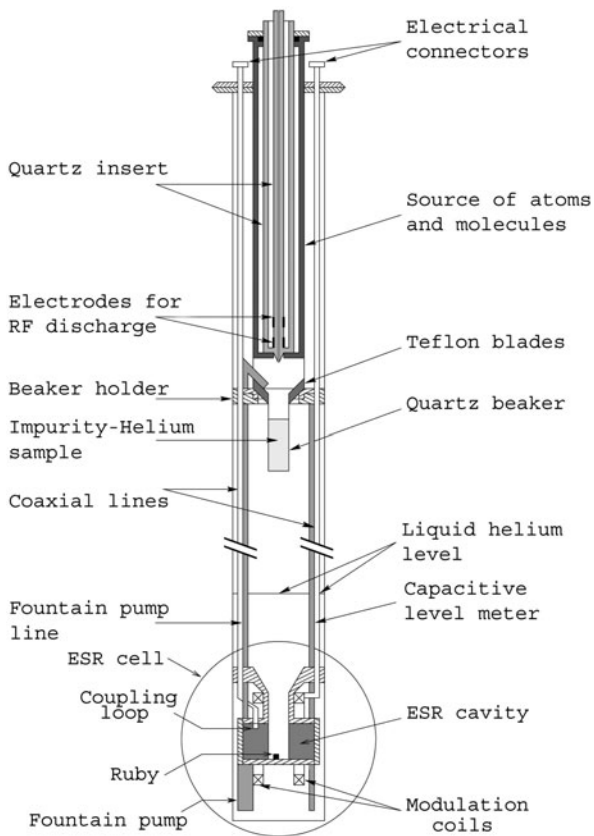
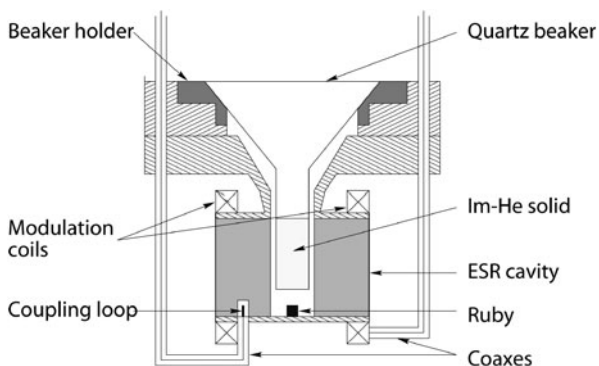
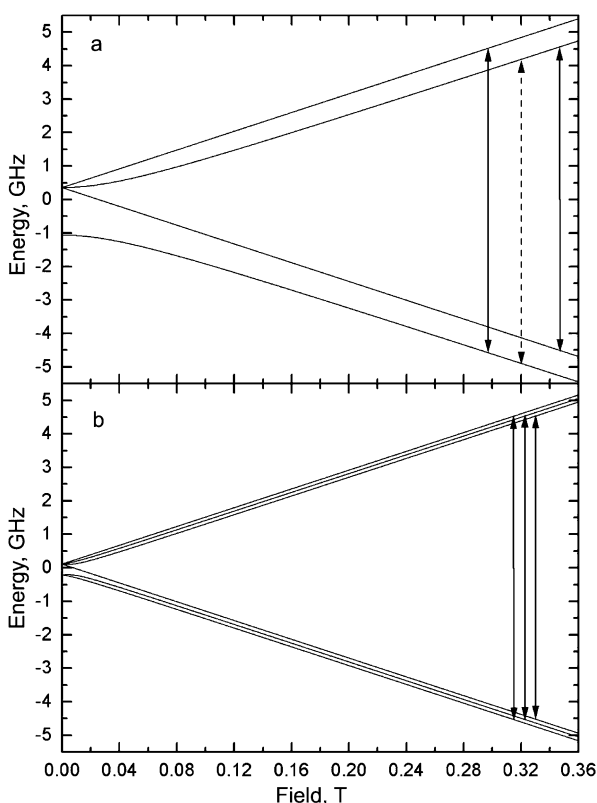


Fig. 3 Diagram of the cell used in the ESR experiments, showing the sample container and TE₀₁₁ resonant cavity operating at 9.07 GHz



to the derivatives of the absorption curves being displayed. A schematic drawing of this cavity is shown in Fig. 3. For reference, the hyperfine diagram of atomic hydrogen is portrayed in Fig. 4a, showing the two allowed ESR transitions separated by approximately 508 Gauss and the forbidden line, which at this applied field is 170 times smaller than the allowed lines. Satellite lines associated with the mutual spin flips between an electron belonging to an atomic hydrogen free radical and a proton of

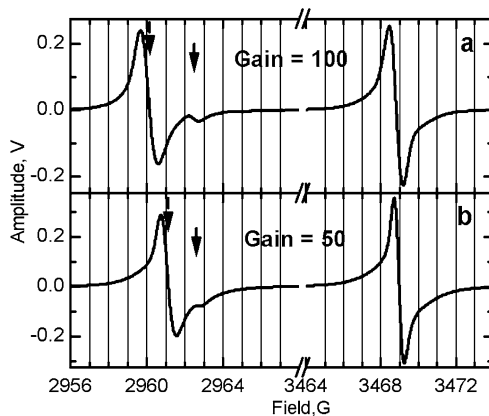
Fig. 4 Energy level diagram for the ground electronic state of hydrogen (a) and deuterium (b) atoms in a magnetic field. The dashed line is the forbidden line of atomic hydrogen



a nearby ortho H_2 molecule or HD molecule can also sometimes be observed. This technique was not effective for deuterium nuclei in the molecules due to the small deuterium magnetic moment. The ESEEM technique discussed in the previous section provided a method to obtain similar information for deuterium. The concentration of the samples was obtained by comparing the line intensity with that of a ruby crystal contained in the cavity. The ruby was in turn calibrated by comparing the ESR line intensity with that of a Diphenyl Picryl Hydrazil sample, which contained a known number of spins. The hyperfine diagram for deuterium atoms is shown in Fig. 4b.

In these experiments, mixtures of hydrogen, krypton and helium gas were admitted into the cryostat and were cryopumped into the low temperature region. En route, they passed through a small orifice, as described in the previous section. A jet emerging from the orifice impinged onto the superfluid helium surface and eventually formed the nanocluster samples inside the sample beaker, which was then lowered into the TE_{011} X band resonant cavity. Figures 5a and 5b show spectra of H atoms prepared from gas mixtures with ratios $\text{H}_2:\text{Kr}:\text{He} = 1:1:200$ and $1:50:10,000$ respectively. A subtle but important difference is observed between the high and low field lines for both samples. The low field line (LFL) exhibited a small but significant bump on the high field wing. No such feature was observed for the high field line (HFL). The field for which the bump was observed was the same for both samples, whereas the positions of the main LFL's were shifted relative to one another by 0.8 Gauss. The

Fig. 5 ESR spectra of H atoms in as prepared H-Kr-He samples at 1.35 K. The *left arrows* point to the positions LFL centers and *right arrows* point to the bump positions. Samples were prepared from gas mixtures with ratios $[H_2]:[Kr]:[He] = 1:1:200$ (a) and $[H_2]:[Kr]:[He] = 1:50:10000$ (b)



data shown in Fig. 5 was taken at 1.35 K. Dramatic changes in the spectra were observed when the samples were heated (annealed) to 14.5 K and then cooled back to 1.35 K. Much of the atomic hydrogen in the samples was lost due to recombination, but the LFL of the remaining hydrogen atoms appeared at a magnetic field which almost exactly coincided with the bump. The position of the HFL did not change appreciably during this process. We interpret these observations in the following way: The bump in the LFL corresponds to H atoms entrapped inside the Kr nanocrystals, whose diameters are ~ 5 nm as measured in previous X-ray diffraction studies [5]. The main LFL line corresponds to H atoms contained in a molecular H_2 film coating the surface of the Kr nanoclusters. The variation of the thickness of the films for the two samples can explain the shifts of the main LFL lines. The main HFL lines were relatively unaffected, with only slight displacements observed. The values of the hyperfine constant A and of the g factor before annealing were determined from the separation between the main LFL and the main HFL by inverting the Breit-Rabi equation [18]. The results gave A values of about 1416 MHz, corresponding closely to the values for H atoms embedded in solid H_2 [19], as compared to the free atom value $A = 1420$ MHz. A similar analysis enabled the hyperfine constants and the g values to be obtained after annealing. Recall that for this case, the LFL occurred exactly at the position of the bump seen for the unannealed samples. The A value found for the bump and also for the annealed sample was approximately 1408 MHz which fits in rather well with the values of 1409 and 1412 MHz for H atoms in substitutional sites of solid Kr [20, 21]. The g values obtained also supported the conclusions reached from considering the values of A for the annealed and unannealed samples. This work has been discussed in detail in recent publications [17, 22], so only the essential features and conclusions are discussed in this presentation.

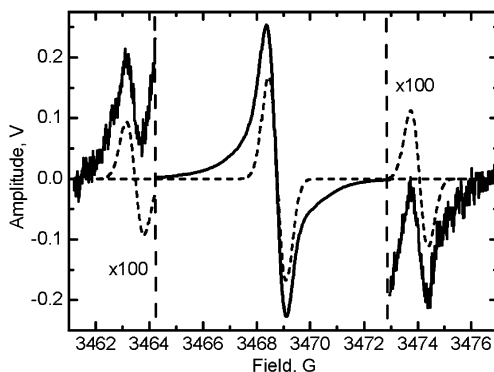
In attempting to explain the large concentrations of H atoms on the Kr cluster surfaces as compared with their concentration in the cluster interiors, we consider the way in which the clusters are formed. The large Van der Waals forces between the Kr atoms lead to the formation of nanoclusters of nearly pure Kr at the early stages of sample preparation, when the jet is at a relatively high temperature as it exits the narrow orifice [22]. As the clusters cool during their descent, the more weakly attracted H atoms, H_2 molecules and He atoms become bound to the cluster surfaces.

We attribute the shift of the main LFLs relative to one another in Fig. 5 to the difference in the initial gas concentrations. This leads to different environments for the H atoms depending on the thickness of the solid H₂ films absorbed onto the Kr surfaces. The sample prepared from the H₂:Kr:He = 1:1:200 corresponds to a thick H₂ film, so any shift of the LFL ESR line due to the influence of the Kr substrate is minimized. On the other hand, the H₂:Kr:He = 1:50:10,000 gas mixture shows a much larger shift from the bare atom LFL, indicating a much greater influence of the Kr substrates, and therefore a much thinner molecular hydrogen film. This conclusion is born out by the fact that the recombination rate is expected to be faster for thicker films. This was indeed the case in our experiments, where the recombination rate for the sample prepared from the 1:1:200 gas mixture was much more rapid than that for the 1:50:10,000 gas mixture. This comes about because the H atoms in the thin films are more strongly bound to the krypton surface, decreasing their mobility, and consequently their recombination rate. The half life for the thick film at 1.35 K was 161 minutes, whereas the thin film sample exhibited virtually no decay. The higher mobility in the thick film sample was a result of the exchange tunneling reaction $H + H_2 \rightarrow H_2 + H$ which allowed H atoms to diffuse through the film. This process is known as chemical diffusion. According to x-ray investigations [5], the density of Kr atoms in Kr-He condensates is of order 10^{20} cm^{-3} . The number of Kr atoms in a cluster with diameter 5 nm is ~ 2000 . This allows one to calculate the concentrations of clusters to be $5 \cdot 10^{16} \text{ cm}^{-3}$. Furthermore, taking into account the average concentrations of H atoms in H₂-Kr-He samples, $1.4 \cdot 10^{18} \text{ cm}^{-3}$, we can estimate that each H₂-Kr cluster should contain ~ 28 stabilized H atoms. Therefore, in our work we are studying mostly recombination of H atoms inside nanoclusters. To achieve a regime for which only one H atom is stabilized in a cluster [24] we need to increase considerably the duration of the experiment. This will allow investigation of the kinetics of the recombination of H atoms from different clusters which would indicate that percolation occurs between clusters [25].

Exchange tunneling chemical reactions were found to take place on samples prepared from the gas mixture HD:Kr:He = 1:5:200. The reaction $D + HD \rightarrow D_2 + H$ was found to occur, as manifested by a decrease in the D atom concentration and an increase in the H atom concentration at 1.35 K. This result proves that the mobility of H and D atoms in our samples was not completely suppressed. The total concentration of atomic free radicals (the sum of the D and H atom concentrations) remained constant throughout the process, indicating that recombination of these atoms into molecules did not occur.

One of the most significant results contained in these experiments was the very high concentration of H atoms achieved. We consider both the average concentration of H atoms, as determined from the ESR signal intensity (corresponding to the double integral of the ESR derivative signal) and their local concentration (determined from the ESR line width). The average concentration can be used to find the total density of the H atoms in the sample, which is much smaller than the corresponding density obtained for a solid formed by compressing the sample and thus eliminating the pores. The average concentration is useful in determining the total chemical energy density stored in the sample. On the other hand, the local density of H atoms allows the average distance between them to be estimated from the dipole-dipole interaction formula for bulk crystals with lattice points randomly populated by atoms with

Fig. 6 A high field main line of atomic hydrogen with satellite lines (*solid lines*). Satellites of the HFL correspond to the Gaussian fitting line. Gaussian fitting lines are presented by *dashed lines*. The sample was prepared from gas mixture $[H_2]:[Kr]:[He] = 1:1:200$ [26]



spin $1/2$, $n = 2.7 \times 10^{19} \times \Delta H_{dd}$ [23]. Since atoms in our samples are mainly localized on the surfaces of the nanoclusters, this formula gives only rough estimation for the lower bound of local densities. The average spacing between the H atoms can be compared with the thermal de Broglie wavelength $\lambda = h/(2\pi mkT)^{1/2}$ for free atoms. When these quantities become comparable in magnitude, quantum overlap starts to occur and quantum statistical correlations may come into play. Furthermore, magnetic ordering and exchange narrowing may also occur as the temperature is lowered.

The average concentration of H atoms for a sample prepared from a gas mixture with the ratio $H_2:Kr:He = 1:1:200$ was 1.4×10^{18} per cm^3 , whereas an estimation for lower bound of the local concentration for this sample was 6×10^{19} per cm^3 as calculated from the line width due to dipolar broadening ($\Delta H = 2.2$ Gauss). Note that λ for a free H atom at $T = 1.35$ K is 1.26 nm as compared with the spacing $d = 2.5$ nm for this sample. The highest average concentration was obtained for the sample prepared from the gas mixture $H_2:Kr:He = 1:50:10,000$ corresponding to a thin molecular H_2 film. The H atom concentration for this sample was 3.2×10^{18} cm^{-3} . This average concentration was increased to 1.2×10^{19} cm^{-3} when the sample was compressed. The typical spacing between H atoms on the Kr nanoclusters with linear dimensions ~ 5 nm was found to be ~ 1.4 nm.

Weak satellite lines were observed on either side of the main HFL (see Fig. 6). The satellite splittings were consistent with the interactions between the unpaired electron spins and the protons on neighboring ortho H_2 molecules. These satellites were observed only for thick films prepared from $H_2:Kr:He$ gas mixtures with the ratios 1:1:200 and 1:1:400.

Studies were also performed on samples prepared from pure deuterium gas along with krypton and helium as discussed by Boltnev et al. [26]. As might be expected, larger average atomic concentrations were achieved for deuterium, with its larger mass. Deuterium samples were prepared from a gas mixture $D_2:Kr:He$ with the ratio 1:5:1200. Most of the experimental samples were fitted by two Lorentzians for each of the three deuterium lines (LFL, HFL and a center line). The three ESR lines are a consequence of the nuclear spin of the deuteron being one, giving six hyperfine levels in a magnetic field. Allowed transition between these levels gives three ESR lines. The two Lorentzian fitting curves for each line typically consisted of a narrow line (width ~ 2 Gauss) and a broad line (width ~ 5.5 Gauss) (see Fig. 7). The 5.5 Gauss

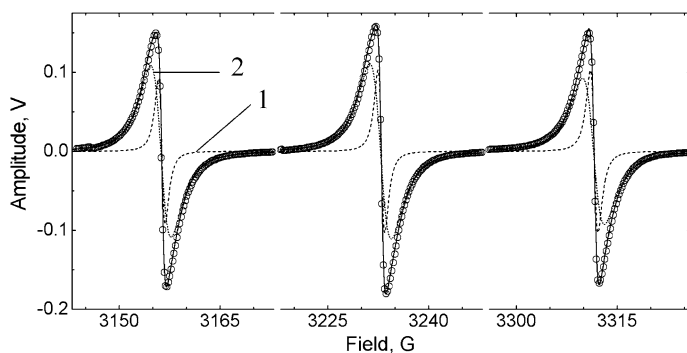


Fig. 7 Experimental ESR spectra of D atoms (*open circles*) in as-prepared Kr-He samples at 1.35 K with three fitting curves for each hyperfine component: 1—narrow Lorentzian, 2—broad Lorentzian, *solid line*—the sum of the fitting lines. Sample was prepared from a gas mixture with ratio $[D_2]:[Kr]:[He] = 1:5:1200$ [26]

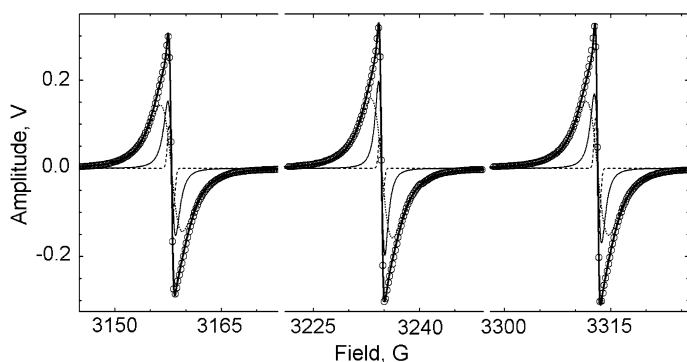


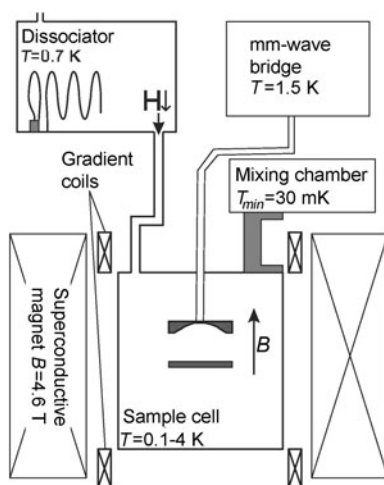
Fig. 8 Experimental ESR spectra of D atoms (*open circles*) in as-prepared Kr-He samples with the highest achieved average concentration of atoms at 1.35 K with three fitting curves for each hyperfine component: narrow Lorentzian—*thin line*, broad Lorentzian—*dotted line*, sharp Gaussian—*dashed line*, the sum of the fitting lines—*thick line*). Sample was prepared from a gas mixture with ratio $[D_2]:[Kr]:[He] = 1:5:1200$ [26]

width Lorentzian indicated a large amount of dipolar broadening, much more than for the largest line width (2.5 Gauss) seen in the experiments with hydrogen atoms. This indicates even higher local concentrations for D atoms than those obtained for H atoms.

There was an important exception, however. The D:Kr:He sample with the highest average concentration of D atoms ($3.3 \times 10^{19} \text{ cm}^{-3}$) showed some sharpening of every triplet component. This can be seen by referring to Fig. 8, showing data at 1.35 K with three fitting curves for each hyperfine component. Two of these fitting curves correspond to the broad and narrow Lorentzians, and the third is a very sharp Gaussian (line width ~ 0.6 Gauss). Clearly, further experimental work will be required to understand this narrowing.

A very significant recent achievement in the field of matrix isolation has been the extension of studies into the temperature region below 1 K. This was first ac-

Fig. 9 Block diagram of the setup for investigations of H atoms in solid H_2 at ultralow temperatures



completed at Turku University in Finland. The studies began with experiments on spin polarized hydrogen atoms adsorbed on the surface of superfluid ^4He by Simo Jaakola's group [27]. More recently, these investigations were extended to measurements on spin polarized hydrogen gas and on hydrogen atoms trapped in thin films (50 nm) of solid molecular hydrogen [28–30]. The samples in all of these experiments were studied by means of mm wave spectroscopy at 4.6 Tesla and 130 GHz. The spectrometer used in this work has been discussed in the first section of this paper. The experiments made use of dilution refrigerators to provide cooling to temperatures below 100 mK. The H atoms were produced in a low temperature radio frequency dissociator and then cryopumped into the sample chamber. All of the inner walls of the sample chamber, dissociator and connecting tubes were coated with a layer of superfluid ^4He to prevent rapid recombination from depleting the H atom population. It should be remarked here that superfluid ^4He films have played a consistent role in preventing recombination on solid surfaces for all of the matrix isolation experiments at Turku, Cornell and Chernogolovka. Figure 9 shows the lower portion of the interior of the vacuum can and the surrounding magnet. The dissociator, the sample cell, as well as the dilution refrigerator mixing chamber, and the heat exchange column are all displayed in this figure. The sample cell contained two Fabry-Perot mirrors. The earliest cavity had two spherical mirrors. A thin Mylar membrane in between the mirrors separated the sample region from a region containing the cold ^3He - ^4He mixture from the dilution refrigerator mixing chamber. This cavity is shown in Fig. 10 along with a schematic of the four hyperfine levels of atomic hydrogen. Later cavities did not have the Mylar membrane and also had one flat mirror and one spherical mirror rather than two spherical mirrors [29, 30]. Several anti-nodes were present in these cavities. The mirror spacings were designed so that the mm wave anti-nodes were at the mirror positions or the Mylar membrane position where the H in H_2 samples were accumulated. The mm waves entered and exited the cavity through a very small hole in one of the mirrors which was connected to a wave guide leading to the spectrometer. Three body recombination of H atoms entering the sample cell yielded a hydrogen molecule and a hydrogen atom with considerable kinetic energy, which

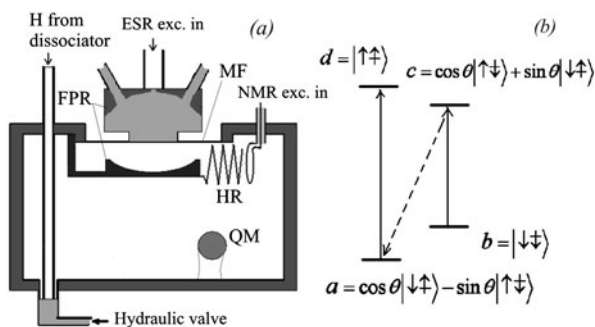


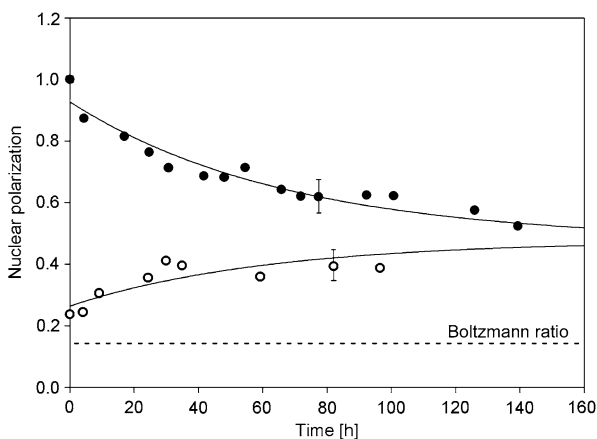
Fig. 10 (a) Schematic drawing of the earliest sample cell. FPR = Fabry-Perot ESR resonator, HR = helical NMR resonator, MF = Mylar foil, QM = quartz microbalance crystal. (b) Hyperfine level diagram for hydrogen atom in a strong magnetic field. Arrows denote electron and nuclear spin projections. The values of the angles θ are determined from the equation $\tan 2\theta = A/[h(\gamma_e + \gamma_p)H]$, where A is the hyperfine constant, H is the magnetic field and γ_e, γ_p are the electron and proton gyromagnetic ratios, respectively [28]

allowed it to penetrate through the superfluid and into the molecular H_2 film. Thus H atoms became lodged in the molecular film. In some of the experiments a quartz microbalance was employed to measure the film thicknesses which were typically of order 50 nm in the early versions of the experiment. The mm wave ESR studies gave H atom concentrations in the films of order 10^{18} cm^{-3} . During sample formation, the ESR signal from the spin polarized hydrogen atomic gas gave a definite absolute frequency value. The ESR lines corresponding to H atoms embedded in the molecular films were shifted from this frequency due to interactions with the surrounding solid H_2 . A helical resonator was placed inside the cell. This resonator was designed to have a resonant frequency corresponding to the transition frequency between the two lowest hyperfine lines of atomic hydrogen. In later experiments [29, 30] this resonator was also operated at higher powers to dissociate H_2 molecules directly inside the sample cell. Cyclotron resonance signals were seen from electrons created by ionizing H atoms in the discharge at these high operating levels.

Recombination studies were performed by observing the mm wave signal amplitudes as a function of time. Second order recombination was found to take place, but the observed rate constants were smaller than predicted by theory for temperatures below 500 mK. At 150 mK the decay was imperceptible over periods exceeding 12 days. The low recombination rates at the lowest temperatures facilitated cooling to lower temperatures.

Saturation could be performed with the mm waves [28], since the H in H_2 lines could be completely saturated by ~ 0.1 nanowatts of excitation power. The a-d line saturation followed a conventional saturation curve. The relaxation time as measured during recovery from full saturation to full signal intensity at low values of H_1 (the mm wave field) was $T_{da} = 3.4 \text{ s}$. The b-c line behaved in an entirely different fashion! After saturation power was applied at the b-c line, and was then reduced, the b-c line remained permanently saturated. The effect is explained as follows: The mm wave power depletes state $|b\rangle$ and adds atoms to state $|c\rangle$. But $|c\rangle$ relaxes rapidly to state $|a\rangle$ in spite of the c-a transition being forbidden. The result is that the population of

Fig. 11 Evolution of the nuclear polarization $p = (n_a - n_b)/(n_a + n_b)$ at $T = 150$ mK after saturation of the b-c transition (closed circles) and after partial saturation of the a-b transition (open circles). The horizontal dashed line marks the nuclear polarization corresponding to a thermal (Boltzmann) ratio $n_a/n_b = \exp(E_{ab}/T)$ with $T = 150$ mK [28]



$|b\rangle$ and $|c\rangle$ are depleted, and in fact, are transferred to state $|a\rangle$. The c-a relaxation time was estimated to be $T_{ca} \leq 5$ sec. This is basically an Overhauser effect.

The helical resonator was particularly useful in ENDOR studies. Referring to the hyperfine diagram in Fig. 10, ENDOR experiments are conducted by depleting the $|b\rangle$ state through saturation of the b-c transition via mm wave excitation and then sweeping the frequency applied to the helical coil through the a-b transition. An absorption signal at the b-c transition frequency was then observed. The ENDOR studies provided an accurate estimate of the hyperfine constant A , which was reduced relative to that of the free atoms, corresponding to the atoms occupying substitutional sites in the solid H₂ film.

The most spectacular result obtained in these experiments is the non-Boltzmann behavior of the populations of the two lowest hyperfine states at the lowest temperatures. The Overhauser effect described above allows one to completely deplete the $|b\rangle$ state since, as we shall see, the a-b relaxation rate is exceedingly slow. Thus the whole population of $|b\rangle$ is transferred to $|a\rangle$ via $|c\rangle$. Over a period of 140 hours at $T = 150$ mK the population of the $|a\rangle$ state relaxes to its equilibrium value. These results are illustrated in Fig. 11. In a separate experiment the a-b transition is partially saturated, giving an excess population in state $|b\rangle$. This is seen to relax over a period of nearly 100 hours toward the same equilibrium value. This equilibrium value does not conform to the Boltzmann distribution. At $T = 150$ mK, the nuclear polarization $p = (n_a - n_b)/(n_a + n_b)$ is 0.5 rather than the value 0.14 expected from the Boltzmann distribution with $n_a/n_b = \exp(E_{ab}/T)$ and $E_{ab} \approx 43$ mK. The same value for the polarization at 150 mK was found following sample formation, after the sample had many hours to relax.

In spite of the long relaxation times for the a-b transition, it was found to be impossible to achieve complete saturation of the a-b line by applying power to the helical coil. This effect is still unexplained. Finally, hole burning experiments were performed by saturating the b-c transition, depleting the $|b\rangle$ state, and allowing transfer of the atoms via the Overhauser effect from state $|c\rangle$ to state $|a\rangle$ at a value of magnetic field corresponding to the peak of the mm wave absorption signal. The $|b\rangle$ state remained depleted at this field value for many hours since the a-b relaxation

time was very long. The excess population of $|a\rangle$ produced in this fashion remained in the $|a\rangle$ state. On the other hand, when a hole burning signal at the peak of the a-d line was applied, the hole lasted only a few seconds, consistent with the a-d relaxation time, T_{ad} .

More recent experiments on H in H₂ films have been performed at Turku by Ahokas et al. [29, 30]. The experiments utilized a cryogenic rf discharge in the sample cell produced by helical resonators to form the H in H₂ films. The densities of H atoms in these experiments exceeded $2 \times 10^{19} \text{ cm}^{-3}$ corresponding to an average separation between the atoms less than 10 lattice constants. Very slow recombination times were reported at low temperatures, even for very dense samples. To explain the effect, Ahokas et al. referred to the work by Kagan and Leggett [12] who considered the energy level mismatches between neighboring lattice sites as the atoms moved closer together. The energy levels were then out of alignment, which kept the atoms from tunneling into close proximity with one another. The recombination rate increased at higher temperatures where the phonon densities were higher. When Ahokas et al. [30] admitted a large number of H atoms into their chamber, the recombination rate increased dramatically due to the increase in phonon density. In a second set of experiments, further measurements were conducted on H atoms trapped in H₂ films by Ahokas et al. ENDOR experiments revealed the presence of two (NMR) lines corresponding to the a-b hyperfine transition.

The temperature dependence of the deviation from the Boltzmann distribution of the populations of the two lowest hyperfine levels of the H atoms was also studied in this more recent work. A spherical mirror with bare metal exposed to the sample was placed on one side of the resonator and a flat mirror covered by Mylar was on the other side. The sample attached to the flat mirror showed a large departure from the Boltzmann distribution at 150 mK in rough agreement (with scatter) with the results of the earlier [28] experiment. On the other hand, the bare spherical mirror gave results which showed behavior more consistent with the Boltzmann distribution. This indicated a possible substrate dependence of the effect.

Jarvinen et al. [31] at Cornell University have performed similar measurements on thicker films. Two closely spaced partially overlapping ESR lines were observed. Jarvinen et al. also used a Fabry–Perot configuration with a flat mirror on one side and a spherical mirror at the other. Data was only taken for the flat mirror, which was coated with Mylar. On this substrate, a strong departure for each of the two component lines from the Boltzmann distribution was obtained in agreement with studies mentioned above. One of the components was rather broad, indicating strong dipolar interactions, and thus a high local concentration, and the other was narrower, indicating a smaller local concentration of H atoms. At higher temperatures, the broader line diminished, indicating a faster recombination rate, leaving only the narrow line.

3 Conclusions

Many problems remain to be addressed in this research area. The deviation from the Boltzmann distribution of the H atoms in the H₂ films needs further study. In particular, are Bose–Einstein correlations in any way involved? The average H atom

concentrations seems too small for Bose–Einstein Condensation (BEC) to take place, but if phase separation occurs, creating regions rich in H atoms and regions more dilute in their H atom populations, it still might be possible. The substrate dependence needs further study, however. Lower temperatures also need to be investigated for this system.

The H:Kr:He and D:Kr:He system should also be in line for further study. The shift of the main low field ESR line of hydrogen with film thickness should be further investigated to determine whether the thickness of the H₂ films on the clusters can be obtained quantitatively by controlling the total amount of hydrogen and krypton admitted into the system. Does the gel like structure allow percolation of the H₂ to occur, which would provide a porous structure through which H atoms could diffuse and interact? If so, could quantum statistical correlations be observed when the H:Kr:He clusters are cooled below 1 K, where the thermal de Broglie wavelength becomes longer? Some of the experimental problems are quite daunting but well worth the effort.

Another challenging problem is the preparation of a population of D atoms embedded in molecular deuterium films and then cooling these samples to 100 mK or less. If such attempts were to be successful, it would provide another test of the hypothesis of BEC for H in H₂, since D atoms obey Fermi-Dirac statistics and would therefore not show manifestations of BEC. On the other hand, Pauli paramagnetism might occur in systems containing high concentrations of deuterium atoms. The small deuteron magnet moments will make such studies quite difficult, however.

An additional promising problem to explore is the possibility of observing spin pair deuterium or hydrogen radicals which corresponds, for example, to a pair of neighboring spins simultaneously flipping from the up to the down position or vice versa. This phenomenon has already been observed at Cornell for pairs of N atoms [32]. The technique employed is to search for an ESR signal at 1/2 the value of the applied steady magnetic field. With a powerful spectrometer, it should be possible to provide an independent measure of the local concentration by studying the saturation curves for the spin pair radicals. The higher the D or H atom concentrations achieved, the greater will be the probability that this phenomenon can be observed.

Exciting ideas are on the horizon in this field of research, but a considerable effort will be required to bring these challenging problems to fruition. Even more support from theorists will be needed as time progresses.

Acknowledgements This work was supported by National Science Foundation Grant DMR 0504683, the Academy of Finland Grants 122595 and 124998, the Wihuri Foundation and the Hackerman Foundation (Project # 010366-0137-2009). We thank Janne Ahokas, Ethan Bernard, Roman Boltnev, Jarno Jarvinen and Carley Paulsen for their strong participation in the recent experiments at Turku and Cornell Universities. We benefited greatly from discussions with Neil Ashcroft, Peter Borbat, Jack Freed, Kaden Hazzard and Erich Mueller.

References

1. A.M. Bass, H.P. Broida, *Formation and Trapping of Free Radicals* (Academic Press, San Diego, 1960)
2. E.B. Gordon, L.P. Mezhev-Deglin, O.F. Pugachev, JETP Lett. **19**, 63 (1974)

3. R.E. Boltnev, E.B. Gordon, V.V. Khmelenko, I.N. Krushinskaya, M.V. Martynenko, A.A. Pelmenev, E.A. Popov, A.F. Shestakov, *Chem. Phys.* **189**, 367 (1994)
4. E.B. Gordon, V.V. Khmelenko, E.A. Popov, A.A. Pelmenev, O.F. Pugachev, *Chem. Phys. Lett.* **155**, 301 (1989)
5. V. Kiryukhin, B. Keimer, R.E. Boltnev, V.V. Khmelenko, E.B. Gordon, *Phys. Rev. Lett.* **79**, 1774 (1997)
6. S.I. Kiselev, V.V. Khmelenko, D.M. Lee, V. Kiryukhin, R.E. Boltnev, E.B. Gordon, B. Keimer, *Phys. Rev. B* **65**, 024517 (2002)
7. E.B. Gordon, A.A. Pelmenev, O.F. Pugachev, V.V. Khmelenko, *JETP Lett.* **37**, 282 (1983)
8. A.V. Ivliev, A.S. Iskovskikh, A.Ya. Katunin, I.I. Lukashevich, V.V. Sklyarevskii, V.V. Suraev, V.V. Filippov, N.I. Filippov, V.A. Shvetsov, *JETP Lett.* **38**, 379 (1983)
9. T. Kumada, *J. Chem. Phys.* **124**, 094504 (2006)
10. S.I. Kiselev, V.V. Khmelenko, D.M. Lee, *Phys. Rev. Lett.* **89**, 175301 (2002)
11. T. Miyazaki, *Atom Tunneling Phenomena in Physics, Chemistry and Biology* (Springer, Berlin, 2004)
12. Y. Kagan, A.J. Leggett, *Quantum Tunneling in Condensed Media* (North-Holland, Amsterdam, 1992)
13. T. Kumada, *Phys. Rev. B* **68**, 052301 (2003)
14. E.P. Bernard, V.V. Khmelenko, D.M. Lee, *J. Low Temp. Phys.* **150**, 516 (2008)
15. S. Vasiliev, J. Jarvinen, E. Tjukanoff, A. Kharitonov, S. Jaakkola, *Rev. Sci. Instrum.* **75**, 94 (2004)
16. J. Jarvinen, C. Paulsen, E.P. Bernard, V.V. Khmelenko, D.M. Lee, *J. Low Temp. Phys.* **152**, 6 (2008)
17. R.E. Boltnev, E.P. Bernard, J. Jarvinen, V.V. Khmelenko, D.M. Lee, *Phys. Rev. B* **79**, 1850506(R) (2009)
18. G. Breit, I.I. Rabi, *Phys. Rev.* **38**, 2082 (1931)
19. C.K. Jen, S.N. Foner, E.L. Cochran, V.A. Bower, *Phys. Rev.* **104**, 846 (1956)
20. S.N. Foner, E.L. Cochran, V.A. Bower, C.K. Jen, *J. Chem. Phys.* **32**, 964 (1960)
21. K. Vaskonen, J. Eloranta, T. Kiljunen, H. Kunttu, *J. Chem. Phys.* **110**, 2122 (1999)
22. R.E. Boltnev, E.P. Bernard, J. Jarvinen, I.N. Krushinskaya, V.V. Khmelenko, D.M. Lee, *J. Low Temp. Phys.* **158**, 468 (2010)
23. C. Kittel, E. Abrahams, *Phys. Rev.* **90**, 238 (1953)
24. E.B. Gordon, *Dokl. Phys. Chem.* **378**, 156 (2001)
25. E.B. Gordon, R. Nishida, R. Nomura, Y. Okuda, *JETP Lett.* **85**, 581 (2007)
26. R.E. Boltnev, V.V. Khmelenko, D.M. Lee, *Low Temp. Phys.* **36**, 484 (2010)
27. S. Vasilyev, S. Jaakkola, *J. Phys. IV France* **116**, 233 (2004)
28. J. Ahokas, J. Jarvinen, V.V. Khmelenko, D.M. Lee, S. Vasiliev, *Phys. Rev. Lett.* **97**, 095301 (2006)
29. J. Ahokas, O. Vainio, J. Jarvinen, V.V. Khmelenko, D.M. Lee, S. Vasiliev, *Phys. Rev. B* **79**, 220505(R) (2009)
30. J. Ahokas, O. Vainio, S. Novotny, J. Jarvinen, V.V. Khmelenko, D.M. Lee, S. Vasiliev, *Phys. Rev. B* **81**, 104516 (2010)
31. J. Jarvinen, V.V. Khmelenko, D.M. Lee, J. Ahokas, S. Vasiliev, *J. Low Temp. Phys.* doi:[10.1007/s10909-010-0317-x](https://doi.org/10.1007/s10909-010-0317-x)
32. V.V. Khmelenko, H. Kunttu, D.M. Lee, *J. Low Temp. Phys.* **148**, 1 (2007)